

# Pulse compression using fiber gratings as highly dispersive nonlinear elements

G. Lenz and B. J. Eggleton

*Bell Laboratories, Lucent Technologies, Murray Hill, New Jersey 07974*

N. Litchinitser

*Institute of Optics, University of Rochester, Rochester, New York 14627*

Received July 7, 1997; revised manuscript received October 7, 1997

Pulse compressors rely on two separate sections. The first section is for bandwidth generation through self-phase modulation and chirp linearization through normal dispersion. In conventional compressors this first section consists of a normal dispersion fiber of appropriate length. The second section is for compensating this linear chirp through anomalous dispersion, typically a prism pair or grating pair. In this way a transform-limited input pulse is compressed into an almost-transform-limited pulse. This scheme is quite different from chirped fiber gratings that are used in reflection to compensate existing chirp: no extra bandwidth is generated and nonlinear effects are not necessary. We propose a scheme for optical pulse compression utilizing an apodized fiber grating in transmission as the nonlinear dispersive element for the first section of the compressor. Near the band edge, on the long-wavelength side of the stop band of the grating, the normal quadratic dispersion is orders of magnitude greater than in a standard optical fiber. Therefore the first section of the compressor may be scaled down in length and the constraints placed on these systems may be relaxed. In this paper we discuss the limitations and the design of such fiber-grating compressors. Analysis and numerical simulation show efficient pulse compression. Further numerical simulation reveals that sufficiently far from the band edge the fiber grating can be modeled as an effective homogeneous medium obeying the nonlinear Schrödinger equation. © 1998 Optical Society of America [S0740-3224(98)01502-1]

OCIS codes: 050.2770, 320.5520, 190.0190, 320.0320.

## 1. INTRODUCTION

Short-pulse propagation in optical fiber in the near-infrared (IR) spectral region is governed mainly by self-phase modulation (SPM) via the Kerr effect and group-velocity dispersion (GVD). The relative strength of these effects is typically given by a characteristic length scale, namely, the dispersion length  $L_D$  and the nonlinear length  $L_{NL}$ , defined as follows<sup>1</sup>:

$$L_D = \frac{\tau_0^2}{s^2 \beta''},$$

$$L_{NL} = \frac{\lambda A_{\text{eff}}}{2 \pi n_2 P}, \quad (1)$$

here  $\tau_0$  is the full width at half-maximum (FWHM) pulse width,  $\beta'' = d^2 \beta / d\omega^2$  is the GVD of the fiber,  $s^2$  is a numerical factor that depends on the pulse shape (2.77 for Gaussian and 3.11 for hyperbolic secant),  $\lambda$  is the wavelength,  $A_{\text{eff}}$  is the effective mode area,  $n_2$  is the nonlinear index, and  $P$  is the peak power of the pulse. The interplay of SPM and GVD leads to important pulse shaping in the fiber: for negative (or anomalous) GVD, soliton effects dominate the pulse evolution. In the positive (or normal) dispersion regime the combined effects of SPM and GVD broaden the pulse spectrum, square the pulse, and produce linear chirp across the entire pulse width, which may then be compensated by a negative dispersion element. Both of these schemes have been used for pulse compression; however, we will discuss mainly the latter

scheme (similar conclusions will apply to soliton compression and can easily be derived).

Compressing a transform-limited pulse requires spectral broadening, which is achieved by use of SPM; however, pure SPM (for nonlinear phase shifts of a few  $\pi$ ) leads to nulls in the pulse spectrum. These nulls cannot be removed by a linear system, and for this reason both SPM and GVD are required in order to achieve the goal of producing compressed pulses close to the transform limit (i.e., of high quality both in the time and the spectral domains). As will be shown, the compression schemes considered here that approach this ideal compression require lengths of fiber that are proportional to the geometric mean of  $L_D$  and  $L_{NL}$ . Since from Eqs. (1)  $L_D \propto \tau_0^2$  and  $L_{NL} \propto \tau_0$  (for fixed pulse energy), the ideal length of the fiber scales as  $L \propto \tau_0^{3/2}$ ; i.e., longer pulses require longer lengths of fiber for efficient compression. In addition, the intrinsic fiber dispersion in standard fiber is very small (usually of the order of 10 ps<sup>2</sup>/km in the IR region), leading to very long dispersion lengths. This implies that, for long input pulses propagating in a standard fiber compressor, the fiber will have to be very long for ideal compression. In this case the peak power has to be scaled down to avoid exceeding the threshold for stimulated Raman scattering, which is detrimental to compression. For example, if the pulse is 10 ps long with a center wavelength of 1.5  $\mu\text{m}$  and propagates in standard fiber, the dispersion length is approximately 5 km. For a pulse energy of 1 nJ, the nonlinear length is approximately 0.5 m, and in this case the Raman threshold is exceeded and a

good compressor is not feasible. Therefore in order to observe nonlinear pulse shaping for pulsewidths of the order of 10–100 ps (e.g., from mode-locked Nd:YAG or semiconductor lasers), in short lengths of fiber, a highly dispersive fiber element is required. Such an element is a fiber grating, where the wavelength of operation is just outside the stopband (photonic gap).

It was pointed out recently that fiber gratings have very large GVD close to the grating stop band.<sup>2–4</sup> This is a direct consequence of the Kramers–Krönig relations: since the grating constitutes a sharp resonance, it is accompanied by strong dispersion. Viewed in another way, the multiple reflections in the grating introduce a time delay that is highly frequency dependent. By operating just outside the stop band, the grating is used in transmission (the passband) and by apodizing the grating, the ripples in the amplitude response can be eliminated. It was shown in Ref. 2 that in typical fiber gratings the GVD could be up to six orders of magnitudes larger than the plain fiber GVD. Obviously this very high dispersion is limited to approximately the bandwidth of the stop band.<sup>3</sup> This increase in GVD reduces the dispersion length from tens of kilometers to a few centimeters. Nonlinear pulse propagation of picosecond pulses in 5-cm-long fiber gratings was recently demonstrated.<sup>4</sup> In these experiments the anomalous dispersion of the gratings was used to study soliton effects in gratings. In this paper we generalize the discussion to include fiber gratings as nonlinear elements with large normal dispersion for applications such as pulse compression (in contrast to previous schemes using only the linear properties of gratings for chirp compensation).

The aim of this paper is to show that efficient pulse compression of picosecond pulses may be achieved by use of very short lengths of fiber with appropriate fiber gratings to produce square pulses with linear chirp across them. These pulses may then be compressed by a linear system with anomalous GVD such as a prism pair, grating pair, or fiber grating device (see Fig. 1). In Section 2 we will review pulse compression based on normal GVD and SPM in a nonlinear dispersive medium followed by a linear dispersive element with anomalous GVD. In Section 3 we will discuss the dispersion characteristics of a grating operating outside the stopband and the implications of the nonnegligible third-order dispersion for pulse compression. In Section 4 we discuss fiber-grating design issues as well as some fundamental limits inherent in this technique. In Section 5 we show the results of numerical simulations.

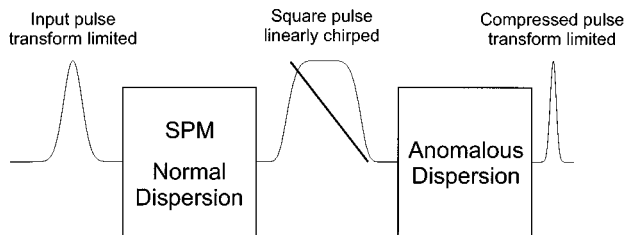


Fig. 1. Schematic drawing of a compressor. The first section generates bandwidth and linear chirp, and the second section compensates this chirp. Ideally the result is an almost-transform-limited compressed pulse.

## 2. PRINCIPLE OF PULSE COMPRESSION

Pulse compression is typically achieved in one of two ways<sup>1</sup>: (1) soliton compression and (2) fiber-grating or fiber-prism compression. The latter method is usually preferred since it yields cleaner compressed pulses, whereas soliton compression is typically accompanied by pedestals on the compressed pulse.<sup>1</sup> As discussed earlier, we will examine the latter method. In this scheme first proposed by Tomlinson,<sup>5</sup> a fiber with positive dispersion is used to broaden the pulse spectrum and generate a square intensity profile with very linear chirp across the pulse. SPM generates new frequencies and broadens the pulse spectrum, and the GVD linearizes the chirp and squares the pulse. The linear chirp can then be compensated by a dispersive element with negative dispersion (such as a grating pair, prism pair, or a chirped fiber grating operating in reflection<sup>6</sup>), producing a nearly-transform-limited compressed pulse. This technique was applied successfully to produce some of the shortest optical pulses.<sup>7</sup> It should be stressed that this method relies on nonlinear effects and spectral broadening, which is in contrast to simple chirp compensation by devices such as chirped gratings. These chirp compensators are linear systems (similar to the second section in our compressor) that do not generate new bandwidth. In the following analysis we will assume linearly polarized pulses and neglect linear and nonlinear birefringence effects.

The pulse-compression technique is governed by two important parameters<sup>1</sup>:

$$N = \sqrt{\frac{L_D}{L_{NL}}},$$

$$z_{\text{opt}} \approx \sqrt{6L_D L_{NL}} \quad \text{for } N \gg 1. \quad (2)$$

The length  $z_{\text{opt}}$  is the optimum length of the fiber (if  $z < z_{\text{opt}}$ , the chirp is not linearized yet, and for  $z > z_{\text{opt}}$  the GVD-induced pulse broadening and corresponding reduction in peak intensity leads to SPM losing its effectiveness), and the best compression results are achieved with a fiber length  $z = z_{\text{opt}}$ . In this case,  $F_c$ , the compression factor, is related to  $N$  through  $N \approx 1.6 F_c$ .

Once the linearly chirped square pulse emerges from the fiber, it needs to have its chirp compensated by an anomalous dispersion element, typically, a grating pair or prism pair, both of which have very small higher-order dispersion and no associated nonlinearity. However, if the nonlinearity is small enough or the peak power is low enough (such that  $L \ll L_{NL}$ ), then a fiber grating may be used since it has anomalous GVD on the short wavelength side of the stopband. It should be emphasized that the nonlinear part of the compressor gives these ideal results when only GVD and SPM are present, i.e., when there is no higher-order dispersion or higher-order nonlinearities. The linear section of the compressor ideally has only negative GVD.

A limiting factor in standard fiber compressors is the threshold for stimulated Raman scattering<sup>1</sup> (SRS). This threshold scales with peak intensity and fiber length; once the threshold is reached, pulse compression degrades significantly. In picosecond duration experiments this usually means using fiber lengths much shorter than

the optimum length ( $L \ll z_{\text{opt}}$ ). In this regime an approximate expression for the compression ratio is given by<sup>5</sup>

$$F_c \approx 1 + 0.6(N^2 L/L_D). \quad (3)$$

This compression factor can be much less than the compression achieved with the optimum fiber length.

### 3. DISPERSION OF FIBER GRATINGS

As was pointed out in the introduction, long lengths of fiber are needed for picosecond pulse compression because of the relatively small fiber dispersion in the near IR. A fiber grating operating in the passband but close to the stop band acts as a highly dispersive element, with a second-order dispersion given by<sup>2</sup>

$$\beta_g'' = -\left(\frac{n}{c}\right)^2 \frac{1}{\delta} \frac{(\kappa/\delta)^2}{[1 - (\kappa/\delta)^2]^{3/2}}, \quad (4)$$

where  $n$  is the linear refractive index,  $c$  is the speed of light, and  $\kappa = \pi \Delta n \eta / \lambda_B$  is the grating coupling coefficient with  $\Delta n$  the index modulation depth,  $\eta$  the fraction of the energy in the fiber core and  $\lambda_B$  the Bragg wavelength.  $\delta = (n/c)(\omega - \omega_B)$  is the detuning parameter with  $\omega_B$  the Bragg frequency. The detuning is positive on the short-wavelength side and negative on the long wavelength, where the GVD is positive. Since we are considering only positive GVD, the detuning will always be negative. To avoid confusion in the following discussion, we will deal with the absolute value of  $\delta$  rather than  $\delta$  itself.

Close to the band edge ( $\delta = \kappa$ ), higher-order dispersion terms cannot be neglected; the cubic dispersion, which is the next coefficient in the Taylor series expansion of the phase (or propagation constant), is given by

$$\beta_g''' = 3\left(\frac{n}{c}\right)^3 \frac{1}{\delta^2} \frac{(\kappa/\delta)^2}{[1 - (\kappa/\delta)^2]^{5/2}}. \quad (5)$$

For efficient pulse compression this cubic term must be minimized. To compare the relative importance of the second- and third-order dispersion, a figure of merit may be defined as follows<sup>1,2</sup>:

$$M = \frac{\beta_g'''}{\beta_g'' \tau_0} = 3 \frac{n}{c \tau_0} \frac{1}{|\delta|} \frac{1}{1 - (\kappa/\delta)^2}. \quad (6)$$

For a given pulse width and grating strength (characterized by  $\kappa$ ), the above relation will yield the detuning required to achieve a certain  $M$ . Note that this definition of  $M$  differs from the definition of  $M_3$  in Ref. 2, by a factor of approximately 1.2.

To demonstrate the effect of third-order dispersion on compression, we add a small amount of cubic dispersion to an ideal compressor (which contains only GVD and SPM) and simulate a 70-ps transform-limited Gaussian input pulse propagating in a homogeneous medium with GVD, SPM, and cubic dispersion. Figure 2 shows the results of this simulation for three values of the  $M$  parameter introduced earlier.  $M = 0$  represents the ideal case of no cubic dispersion, and  $M = 0.1$  and  $0.05$  are also shown (as a point of reference: for standard fiber with

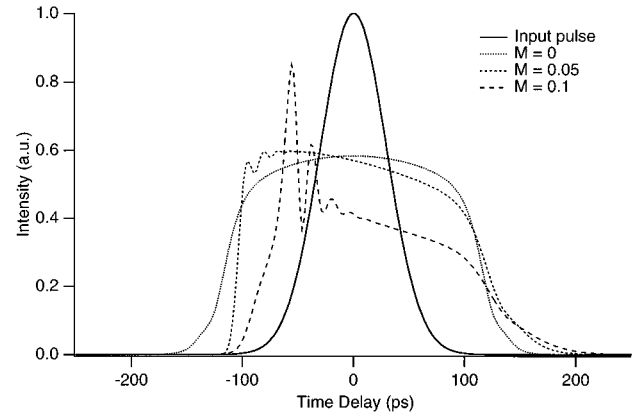


Fig. 2. Effect of cubic dispersion on the compressor performance.  $M$  is a measure of the relative magnitude of quadratic and cubic dispersion (see text). This simulation assumes a 70-ps Gaussian pulse of 170-GW/cm<sup>2</sup> peak intensity propagating in a 10-cm homogeneous medium with  $\beta_2 = 50$  ps<sup>2</sup>/cm and  $\beta_3 = 0$ ,  $\beta_3 = 175$ , and  $\beta_3 = 350$  ps<sup>3</sup>/cm for  $M = 0$ ,  $M = 0.05$ , and  $M = 0.1$ , respectively.

the same input pulse  $M = 7 \times 10^{-5}$ ). As can be seen, third-order dispersion introduces pulse asymmetry as well as structure on the leading edge, which will cause some trailing energy on the compressed pulse. A reasonable  $M$  value is therefore  $< 0.05$ . As an example, we consider a pulse width of 70 ps and a grating strength of  $\kappa = 100$  cm<sup>-1</sup> (corresponding to a  $\Delta n = 0.004$ ,  $\lambda_B = 1.06$   $\mu$ m, and  $\eta = 80\%$ ); using  $M = 0.05$  in Eq. (6) yields a detuning parameter of 123 cm<sup>-1</sup> (which corresponds to a 1.5-nm shift relative to the Bragg wavelength). We can now use Eq. (4) to calculate the second-order dispersion and we get  $\beta_g'' = 64$  ps<sup>2</sup>/cm, which is about  $3 \times 10^5$  larger than standard fiber at this wavelength. This in turn means that the dispersion length is scaled down from kilometers to centimeters.

We emphasize the following points: (1) The above relations are for a grating operating in transmission (i.e., in the passband). (2) This dispersive behavior of the grating outside the stop band is similar to the strong dispersion found near any sharp resonance. (3) It is clear that because of the proximity of the resonance, very high dispersion may be achieved relative to the material dispersion of fiber, which is the result of very far resonances. (4) In order to avoid complications resulting from the side lobes in the grating response, apodization of the grating may be used to remove these side lobes. (5) The dispersion at the wavelength of operation may be tuned to some extent by applying heat or strain to the grating, which changes the linear index and therefore the detuning parameter and the dispersion. These properties show the fiber grating to be a very versatile and useful dispersive element. We next discuss the application of such a fiber grating for picosecond pulse compression.

### 4. PULSE-COMPRESSION DESIGN

The general design criteria are limited by two factors: the peak intensity and the higher-order dispersion. High peak intensity is detrimental because it leads to (1) SRS, (2) shifting of the Bragg resonance (similar to the optical

Stark effect) and to an intensity-dependent dispersion close to the stop band, and (3) truncation of the initial pulse spectrum that gets broadened by SPM: if the broadening is larger than the detuning parameter, the spectrum will get clipped by the grating. Finally, higher-order dispersion leads to pulse distortion as shown earlier; however, if this higher-order dispersion is also compensated by the compensating section, this may not be a problem. We now examine the limits imposed by these different effects on the design of the fiber grating.

The threshold for SRS dictates an upper limit on the product of peak power and fiber length as follows<sup>1</sup>:

$$\frac{g_R P L_{\text{eff}}}{A_{\text{eff}}} < 16 \Rightarrow PL < \frac{16 A_{\text{eff}}}{g_R}, \quad (7)$$

where  $g_R$  is the Raman gain coefficient at the wavelength of operation and  $L_{\text{eff}}$  is the effective length limited by loss. In our case the lengths of interest are such that  $L_{\text{eff}} \approx L$ . This leads to a lower limit on the nonlinear length defined in Eq. (1):

$$L_{\text{NL}} > \frac{g_R \lambda}{32 \pi n_2} L. \quad (8)$$

The limit expressed in relation (8) is a general limit for this type of compressor and therefore is not related to the grating parameters. The next two limits to be discussed are specific to fiber gratings: (1) an intensity-dependent shift of the Bragg resonance leading to nonlinear dispersion. As is shown in the appendix, for  $\kappa \ll \delta_0$ ,  $L_{\text{NL}} \delta_0 \ll 1$  is required to minimize this effect (here  $\delta_0$  is the low-intensity detuning parameter).

The last limitation imposed by the peak intensity is due to SPM-induced spectral broadening of the input pulse spectrum. This broadening factor will be approximately  $F_c$ , since this is the intended purpose of the compressor. We now have to ensure that this spectrum does not overlap the reflection spectrum of the grating, since this would cause the spectrum to be clipped. The input bandwidth (FWHM) of a transform-limited Gaussian pulse of width (FWHM)  $\tau_0$  is given by  $\Delta\nu = 0.441/\tau_0$ , and the output spectral bandwidth is approximately  $0.441 F_c/\tau_0$ . Half of this spectral bandwidth must be smaller than the spectral distance from the band edge ( $|\delta| = \kappa$ ):

$$|\delta| - \kappa > \frac{2\pi n}{c} 0.22 \frac{F_c}{\tau_0} = 1.39 \frac{n}{c \tau_0} F_c = \frac{1.39}{l} F_c, \quad (9)$$

where  $l$  is the spatial length of the pulse in the fiber at the input of the grating.

Finally we consider a purely linear property of the grating, namely, the higher-order dispersion. As shown earlier, this limitation comes from the figure of merit  $M$ . Using Eq. (6), we get a lower limit on the detuning parameter (given the grating strength):

$$|\delta| > \frac{3n}{2M\tau_0 c} + \left[ \left( \frac{3n}{2M\tau_0 c} \right)^2 + \kappa^2 \right]^{1/2}, \quad (10)$$

which in turn will put an upper limit on the GVD. If we define  $\delta_c$  as the limiting value above, the upper limit on the GVD can be written as

$$\beta'' < \left( \frac{n}{c} \right)^{1/2} \left( \frac{M\tau_0}{3\delta_c} \right)^{3/2} \kappa^2. \quad (11)$$

We can now place a lower limit on the dispersion length by using its definition [Eq. (1)]:

$$L_D > \left( \frac{c}{n} \right)^{1/2} \left( \frac{3\delta_c}{M} \right)^{3/2} \frac{\sqrt{\tau_0}}{\kappa^2 s^2}. \quad (12)$$

Since the compression factor scales with  $N$ , it is clear that for maximum compression we would like to operate at the lower limit of the nonlinear length and at the same time maximize the dispersion length. However, by increasing the dispersion length, the optimum length will increase, and we are limited by the grating lengths that are technologically feasible. A good measure would be the ratio of the optimum length [as defined in Eq. (2)] and the grating length  $L$ :

$$q \equiv \frac{z_{\text{opt}}}{L} \approx \left[ 6 \left( \frac{L_D}{L} \right) \left( \frac{L_{\text{NL}}}{L} \right) \right]^{1/2}. \quad (13)$$

The SRS-imposed limit is the strictest one since it involves only material parameters and the wavelength of operation (the other intensity-dependent limitations may be avoided by careful grating design). In this case,  $q$  will be determined by the normalized dispersion length  $L_D/L$  and will increase with a square-root dependence. Since ideally we would like  $q = 1$ , this will put an upper limit on the dispersion length. In particular for  $q \gg 1$ , the compression factor is given approximately by  $1 + 0.6N^2(L/L_D)$  rather than  $N/1.6$ . We will therefore restrict ourselves to  $q$  values not much larger than 1, and using Eq. (13) with the definition of the compression factor  $F_c$ , we can finally write an absolute upper limit for the compression ratio:

$$F_c \approx \frac{N}{1.6} = \frac{q}{1.6\sqrt{6}} \frac{32\pi n_2}{\lambda g_R} = 25.65q \frac{n_2}{\lambda g_R}. \quad (14)$$

Note that the above relation holds for this type of compression in general and does not contain any grating parameters. Ideally we would like to design a grating that achieves this compression ratio and that has a reasonable length.

## 5. NUMERICAL EXAMPLES

We now look at the parameters required for pulse compression of a 60-ps Gaussian pulse with a center wavelength of 1.06  $\mu\text{m}$ . At this wavelength the measured value of the Raman gain (at  $\lambda = 1 \mu\text{m}$ ) is  $g_R = 10^{-11} \text{ cm/W}$  and  $n_2 = 2.6 \times 10^{-16} \text{ cm}^2/\text{W}$ , so for  $q = 1$  the upper limit on the compression factor as given by Eq. (14) is  $\sim 6.3$ . We will outline the design parameters for a grating that will enable a compression of  $F_c \approx 5$ . It has been demonstrated experimentally<sup>8</sup> that the Raman threshold for a 60-ps pulse at 1.06  $\mu\text{m}$  propagating through 10 m of fiber is  $\sim 1 \text{ kW}$ , so for grating lengths of up to 1 m an input peak power of 10 kW may be used. The corresponding nonlinear length (for an effective mode area of 50  $\mu\text{m}^2$ ) is  $L_{\text{NL}} = 3.2 \text{ cm}$ , which may be used as a lower limit. In order to get a compression factor of 5, we use  $L_D = 207.4 \text{ cm}$  (with a corresponding GVD of

6.3 ps<sup>2</sup>/cm) and an optimum length of 63.5 cm. By choosing the detuning  $\delta = -80 \text{ cm}^{-1}$  and the grating strength  $\kappa = 32.4 \text{ cm}^{-1}$ , we get an  $M$  parameter of 0.04 (with a cubic dispersion term of 13.6 ps<sup>3</sup>/cm). It can easily be verified that all these numbers are within the limits outlined in the previous section. Recently, 1-m-long gratings have been demonstrated,<sup>9</sup> so that a 63.5-cm grating is feasible. A shorter grating of 20 cm will degrade the compression factor by less than 10%.

Using these parameters, we simulated numerically the propagation in two different ways: (1) a full numerical solution of the nonlinear coupled equations for the apodized grating<sup>10</sup> and (2) a split-step Fourier method through a homogeneous medium with the above material parameters. In both cases we look at the output pulse before the compensating section. In Figs. 3(a) and 3(b) we show the input and output pulses, respectively, in the time and frequency domains, and in Fig. 3(c) we show the pulse and the chirp across it just before the compensating section. As can be seen, the compressed pulse has some residual trailing energy in the time domain and a small ripple in its spectrum (both consequences of the small third-order dispersion) but is still of reasonably high quality. In this case we used the simpler split-step routine. Figure 4 compares the results of the two different simulation methods using the same parameters but with a grating length of 20 cm. Figure 4(a) shows the intensity profile of the pulse before the dispersion compensating

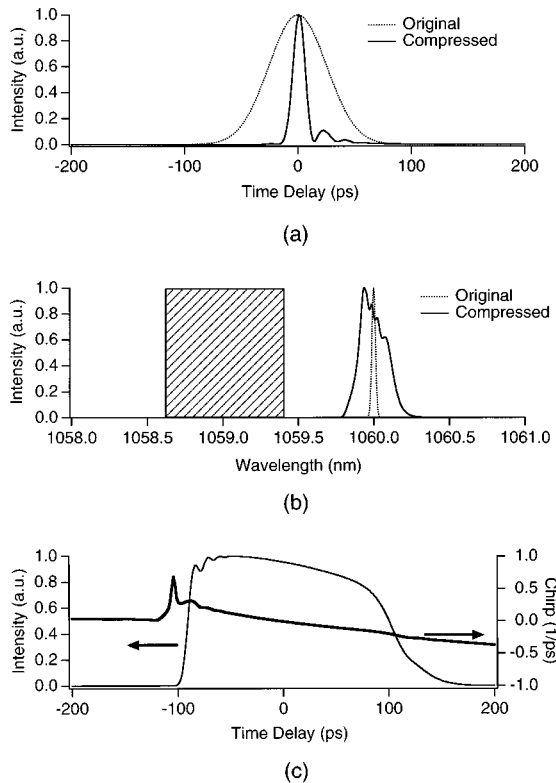


Fig. 3. (a) Input 60-ps transform-limited Gaussian pulse of 20-GW/cm<sup>2</sup> peak intensity and the final compressed pulse. (b) The corresponding spectra; the location and width of the stop band are indicated by the hatched region. (c) The pulse and its chirp after propagating through 63.5 cm of a homogeneous medium with  $\beta_2 = 6.3 \text{ ps}^2/\text{cm}$  and  $\beta_3 = 13.6 \text{ ps}^3/\text{cm}$ .

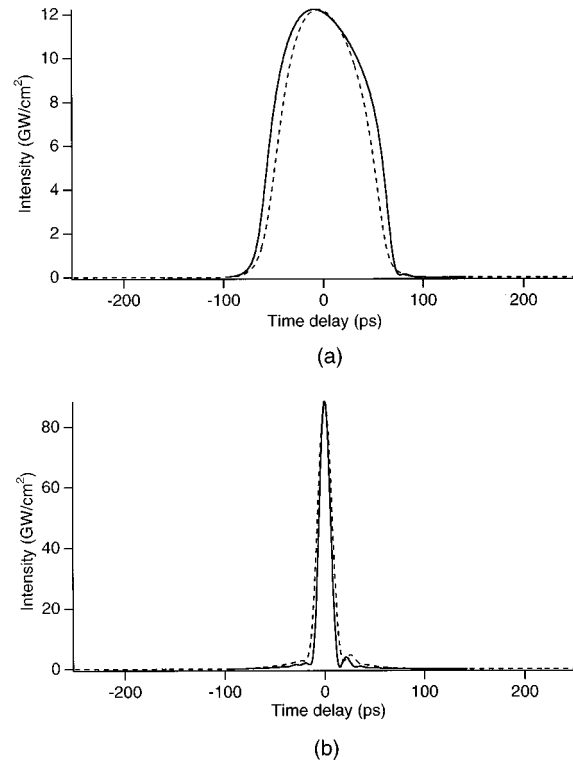


Fig. 4. Comparison of simulation results using the split-step Fourier method (dashed curve) and the full nonlinear coupled-mode equations for gratings (solid curve), for (a) the pulse intensity profile before and (b) after the dispersion-compensating section.

section, and Fig. 4(b) shows the resulting compressed pulse at the output of the system with a compression factor of 4.6.

The close agreement between the two simulation methods demonstrates that far from the stop band, the grating may be viewed as an effective homogeneous nonlinear dispersive medium to which the nonlinear Schrödinger equation may be applied. This is a significant simplification for numerical calculations since the split-step Fourier method is simpler to implement and is much faster. This nonlinear Schrödinger approximation is valid when the pulse is far enough in spectrum from the gap such that their interaction is small. This may be quantified by the spectral bandwidth (i.e., the pulse spectrum should be a few bandwidths away from the edge of the gap) and the peak intensity ( $\delta L_{NL} \gg 1$ ; see appendix).

## 6. CONCLUSIONS

In this paper we have introduced a fiber grating as a highly dispersive nonlinear element for use in a fiber compressor. Previous schemes using gratings mainly in reflection were used for chirp compensation (the initial and final pulse have the same bandwidth) and therefore as linear elements. In other words they can be used only for the second section of the compressor described in this paper.

The main ingredient in the scheme we propose is the very large normal dispersion achievable in the passband of fiber gratings on the long-wavelength side of the stop-

band edge. This scheme becomes particularly appealing for the compression of 10–100 ps, since very long optical fibers may be replaced with very short apodized fiber gratings. We have presented analysis of the limitations placed on this system mainly by higher-order dispersion terms and high peak intensities. Numerical simulations show the performance predicted by analysis as well as the close agreement between the results of the full nonlinear coupled-mode equations and the simple split-step Fourier propagation scheme with the grating modeled as an effective homogeneous medium. This indicates that far enough from the band edge the nonlinear Schrödinger equation may be used with the dispersion terms given by Eqs. (4) and (5).

The second part of the compressor is a linear system that performs chirp compensation and could also be done with a fiber grating (uniform or chirped) either in transmission (on the short-wavelength side of the stop band)<sup>2,11</sup> or in reflection.<sup>6</sup> In this section, nonlinear effects need to be negligible, and therefore the intensity of the pulse emerging from the first section would need to be attenuated. This, of course, is unnecessary when prism or grating pairs are used. Recently, however, gratings in chalcogenide fibers have been reported.<sup>12</sup> These fibers have a very large nonlinear index in the near IR (up to 100 times that of silica at similar wavelengths), which in turn would require much lower intensities. This suggests an all-fiber compressor where the first section would be a chalcogenide fiber grating and the second section would be a standard fiber grating (in which the nonlinear effects would be negligible because of the scaled-down intensities in the chalcogenide fiber). Note also that for chalcogenide fiber the upper limit on compression given by Eq. (14) would be much higher (assuming the Raman gain is similar).

Finally, we note that for the compression of very short pulses this scheme holds no advantages over standard fiber. The reason for this is the scaling of the ideal length with pulse width, which, as was mentioned earlier, is  $\tau_0^{3/2}$  for fixed pulse energy. This means that going from an initial pulse width of 100 ps to 1 ps, the ideal fiber length decreases by a factor of 1000 to a length of only a few meters, avoiding SRS and making a plain fiber more practical. Also, the increase in pulse bandwidth will require operation further from the band edge to achieve a given  $M$  value, which will lead to a larger dispersion length and a longer grating.

## APPENDIX A

In this appendix we analyze the effects of nonlinear dispersion that results from intensity-dependent shifts in the Bragg wavelength,  $\lambda_B = 2n\Lambda$ , where  $\Lambda$  is the grating periodicity and  $n$  is the effective linear index. To first order in intensity, the grating strength  $\kappa$  is intensity independent, since it is proportional to  $\Delta n/n$  (rather than  $n$ ). In other words, to this order, the stop-band width does not change (only its position changes). Through the change in the Bragg wavelength the detuning parameter  $\delta$  changes as follows:

$$\delta(I) = \pi \left( \frac{2n}{\lambda} + \frac{2n_2 I}{\lambda} - \frac{1}{\Lambda} \right) = \delta_0 + \frac{2\pi n_2 I}{\lambda}, \quad (15)$$

where  $\delta_0$  is the linear or intensity-independent detuning. Both the second- and third-order dispersion depend on the refractive index and on the detuning parameter and are therefore intensity dependent. To first order in intensity, the second- and third-order dispersion are given by

$$\begin{aligned} \frac{\beta''(I)}{\beta''(0)} &= 1 - \frac{2\pi}{\lambda} n_2 I \frac{1}{\delta_0} \frac{3}{1 - (\kappa/\delta_0)^2} \\ &= 1 - \frac{1}{L_{\text{NL}}\delta_0} \frac{3}{1 - (\kappa/\delta_0)^2}, \\ \frac{\beta'''(I)}{\beta'''(0)} &= 1 - \frac{2\pi}{\lambda} n_2 I \frac{1}{\delta_0} \frac{4 + (\kappa/\delta_0)^2}{1 - (\kappa/\delta_0)^2} \\ &= 1 - \frac{1}{L_{\text{NL}}\delta_0} \frac{4 + (\kappa/\delta_0)^2}{1 - (\kappa/\delta_0)^2}. \end{aligned} \quad (16)$$

From the above relations it is obvious that in order to minimize the effects of nonlinear dispersion we need to maximize the product  $L_{\text{NL}}\delta_0$ , which means increasing the detuning or decreasing the intensity so that the intensity-dependent correction is negligible (say <1%).

## REFERENCES

1. G. P. Agrawal, *Nonlinear Fiber Optics* (Academic, San Diego, 1989).
2. N. M. Litchinitser, B. J. Eggleton, and D. B. Patterson, "Fiber Bragg gratings for dispersion compensation in transmission: theoretical model and design criteria for nearly ideal pulse compression," *J. Lightwave Technol.* **15**, 1303–1313 (1997).
3. P. St. J. Russell, "Bloch wave analysis of dispersion and pulse propagation in pure distributed feedback structures," *J. Mod. Opt.* **38**, 1599–1619 (1991); Erratum, *J. Mod. Opt.* **41**, 163–164 (1994).
4. B. J. Eggleton, R. E. Slusher, C. M. de Sterke, P. A. Krug, and J. E. Sipe, "Bragg grating solitons," *Phys. Rev. Lett.* **76**, 1627–1630 (1996); B. J. Eggleton, C. M. de Sterke, and R. E. Slusher, "Nonlinear pulse propagation in Bragg gratings," *J. Opt. Soc. Am. B* **14**, 2980–2993 (1997).
5. W. J. Tomlinson, R. H. Stolen, and C. V. Shank, "Compression of optical pulses chirped by self phase modulation in fibers," *J. Opt. Soc. Am. B* **1**, 139–143 (1984).
6. J. A. R. Williams, I. Bennion, and L. Zhang, "The compression of optical pulses using self-phase-modulation and linearly chirped Bragg-gratings in fibers," *IEEE Photonics Technol. Lett.* **7**, 491–493 (1995).
7. R. L. Fork, C. H. Brito Cruz, P. C. Becker, and C. V. Shank, "Compression of optical pulses to six femtoseconds by using cubic phase compensation," *Opt. Lett.* **12**, 483–485 (1987).
8. E. M. Dianov, A. Ya. Karasik, P. V. Mamyshev, G. I. Onishchukov, A. M. Prokhorov, M. F. Stel'makh, and A. A. Fomichev, "Picosecond structure of the pump pulse in stimulated Raman scattering in a single-mode optical fiber," *JETP Lett.* **39**, 691–695 (1984).
9. L. Dong, M. J. Cole, A. D. Ellis, M. Durkin, M. Ibsen, V. Gusmeroli, and R. I. Laming, "40 Gbit/s 1.55  $\mu\text{m}$  transmission over 109 km of non-dispersion shifted fibre with long continuously chirped fibre gratings," presented at the Optical Fiber Communication Conference of the Optical Society

- of America, Dallas, Texas, February 16–21, 1997, postdeadline paper PD6.
10. C. M. de Sterke, K. R. Jackson, and B. D. Robert, "Nonlinear coupled mode equations on a finite interval: a numerical procedure," *J. Opt. Soc. Am. B* **8**, 403–412 (1991).
  11. B. J. Eggleton, T. Stephens, P. A. Krug, G. Dhosi, Z. Brod- zeli, and F. Ouelette, "Dispersion compensation over 100 km at 10 Gbit/s using a fiber grating in transmission," *Electron. Lett.* **32**, 1610–1611 (1996).
  12. M. Asobe, "Nonlinear optical properties of chalcogenide glass fibers and their application to all-optical switching," *Opt. Fiber Technol.* **3**, 142–148 (1997).